Electronic Transactions on Numerical Analysis.
Volume 41, pp. 109-132, 2014.

ISSN 1068-9613.

ETNA
Kent State University
http://etna.math.kent.edu

ERROR ESTIMATES FOR A TWO-DIMENSIONAL SPECIAL FINITE ELEMENT METHOD BASED ON COMPONENT MODE SYNTHESIS*

ULRICH HETMANIUK† AND AXEL KLAWONN‡

Abstract. This paper presents a priori error estimates for a special finite element discretization based on component mode synthesis. The basis functions exploit an orthogonal decomposition of the trial subspace to minimize the energy and are expressed in terms of local eigenproblems. The a priori error bounds state the explicit dependency of constants with respect to the mesh size and the first neglected eigenvalues. A residual-based a posteriori error indicator is derived. Numerical experiments on academic problems illustrate the sharpness of these bounds.

Key words. domain decomposition, finite elements, eigendecomposition, a posteriori error estimation

AMS subject classifications. 35J20, 65F15, 65N25, 65N30, 65N55

1. Introduction. Classical Lagrangian finite element methods are challenged by problems

$$
\begin{aligned}
-\nabla \cdot (\mathbf{A}(\mathbf{x})\nabla u(\mathbf{x})) &= f(\mathbf{x}) \qquad \text{in } \Omega,\\
u &= 0 \qquad \text{on } \partial\Omega,
\end{aligned}
\tag{1.1}
$$

where the coefficient matrix $\mathbf{A}$ is *rough* or *highly oscillating* so that a standard application of the finite element method needs a highly refined mesh to reach sufficient accuracy. Over the last couple of years, many discretization methods have been proposed to enable the accurate, efficient, and robust solution of these complex problems. Approximation subspaces that incorporate specialized knowledge of the coefficient matrix $\mathbf{A}$ give rise to effective finite element methods. Examples include the multiscale finite element [15, 21], the mixed multiscale finite element [1], the heterogeneous multiscale finite element [14], adaptive multiscale methods [28], and the generalized finite element method [3, 4, 6]. Babuška, Caloz, and Osborn [5, p. 947] denote such finite element methods *special*.

Hetmaniuk and Lehoucq [20] proposed to build a conforming approximation space by local eigenfunctions for the partial differential operator in (1.1). Eigenbases are often efficient in terms of Kolmogorov *n*-width (see Melenk [26]), and local eigenfunctions are supposed to span a good approximation space. The discretization in [20] is based upon the classic idea of component mode synthesis (CMS), introduced in [13, 23] and used, e.g., by Gervasio et al. [16] in the spectral projection decomposition method. Starting from a partition of the domain Ω, component mode synthesis methods exploit an orthogonal decomposition of $H_0^1(\Omega)$ to solve the minimization problem

$$
\underset{v\in H_0^1(\Omega)}{\operatorname{argmin}} \left(\frac{1}{2}\int_\Omega (\nabla v(\mathbf{x}))^T \mathbf{A}(\mathbf{x})\nabla v(\mathbf{x})\, d\mathbf{x} - \int_\Omega f(\mathbf{x})v(\mathbf{x})\, d\mathbf{x} \right).
\tag{1.2}
$$

For two-dimensional problems, the conforming approximation space proposed in [20] combines *bubble eigenfunctions* (localized inside one element), energy-minimizing extensions of *vertex-specific* trace functions (localized on the elements sharing the vertex), and energy-minimizing extensions of *edge-bubble eigenfunctions* (localized on an edge and the adjacent elements). Numerical experiments in [20, 24] illustrate the efficacy of this CMS-based

*Received August 17, 2013. Accepted March 28, 2014. Published online on June 20, 2014. Recommended by Y. Achdou. The work is partly supported by NSF grant DMS-0914876.

†Department of Applied Mathematics, University of Washington, Box 353925, Seattle, WA 98195 (hetmaniu@uw.edu).

‡Mathematisches Institut, Universität zu Köln, Weyertal 86-90, 50931 Köln, Germany (klawonn@math.uni-koeln.de).

ETNA
Kent State University
http://etna.math.kent.edu

approach. The first goal of this paper is to present a priori error estimates for this local eigenfunction-based discretization. The error bounds state the explicit dependency of constants with respect to the mesh size and the first neglected eigenvalues.

Special finite element methods allow great flexibility in their definition. These numerical methods often contain a parameter, such as the *vertex-specific* trace function or the number of eigenfunctions, motivated by heuristics arguments. An efficient choice of parameter(s) may not be known in advance and could be estimated adaptively during the computations. The second objective of this paper is to derive an a posteriori error indicator that could guide the selection of the number of *bubble eigenfunctions* and *edge-bubble eigenfunctions*.

The rest of the paper is organized as follows. Section 2 reviews notations and the local eigenfunction-based discretization. Section 3 presents a priori error estimates and a residual-based a posteriori error indicator. Finally, numerical experiments illustrate the sharpness of these bounds.

2. Review of a special finite element method based on component mode synthesis. Let Ω be a bounded polygonal domain in the plane $\mathbb{R}^2$ whose boundary $\partial\Omega$ is composed of straight lines. On this domain, the Sobolev spaces $H^k(\Omega)$ and $H_0^k(\Omega)$ are defined in a standard way (with $k > 0$). Fractional order Sobolev spaces $H^s(\Omega)$ are defined by interpolation. Denote

$$a(u,v) = \int_\Omega (\nabla u(\mathbf{x}))^T \mathbf{A}(\mathbf{x}) \nabla v(\mathbf{x}) d\mathbf{x} \qquad \forall u,v \in H_0^1(\Omega),$$

the bilinear form induced by (1.1). The coefficient matrix $\mathbf{A}$ is assumed to be symmetric positive definite, to be C^1 on $\overline{\Omega}$, and to satisfy

$$0 < \alpha_{\min} \boldsymbol{\xi}^T \boldsymbol{\xi} \leq \boldsymbol{\xi}^T \mathbf{A}(\mathbf{x}) \boldsymbol{\xi} \leq \alpha_{\max} \boldsymbol{\xi}^T \boldsymbol{\xi} \qquad \forall \mathbf{x} \in \overline{\Omega} \text{ and } \boldsymbol{\xi} \in \mathbb{R}^2 \setminus \{\mathbf{0}\}. \tag{2.1}$$

Given $f \in L^2(\Omega)$, the problem (1.2) is rewritten as

$$\operatorname*{argmin}_{v \in H_0^1(\Omega)} \left(\frac{1}{2} a(v,v) - (f,v) \right),$$

where $(\cdot,\cdot)$ denotes the standard inner product on $L^2(\Omega)$. The associated optimality system is the variational formulation of (1.1): find $u \in H_0^1(\Omega)$ such that

$$a(u,v) = (f,v) \quad \forall v \in H_0^1(\Omega). \tag{2.2}$$

We refer to the solutions of (1.1), (1.2), and (2.2) as equivalent in a formal sense. Throughout the paper, the regularity assumption is:

ASSUMPTION 1. Given $f \in L^2(\Omega)$, there exists $s_0 > \frac{3}{2}$ such that the solution u belongs to $H^{s_0}(\Omega) \cap H_0^1(\Omega)$.

This regularity assumption implies some conditions for the domain Ω. For example, when Ω is convex, Assumption 1 holds with $s_0 = 2$; see Grisvard [17, Theorem 3.2.1.2].

Consider a family $(\mathcal{T}_h)_h$ of conforming partitions of Ω into a finite number of triangles or convex quadrilaterals with straight edges. The mesh size h is the maximal diameter of the elements K in $\mathcal{T}_h$. Here every element K is assumed to be a non-empty bounded open set. The family $(\mathcal{T}_h)_h$ is assumed to be shape regular, i.e., the ratio of the diameter of any element K in $\mathcal{T}_h$ to the diameter of its largest inscribed ball is bounded by a constant σ independent of K and of $\mathcal{T}_h$. The interface Γ is defined as

$$\Gamma = \left(\bigcup_{K \in \mathcal{T}_h} \partial K \right) \setminus \partial\Omega.$$

ETNA
Kent State University
http://etna.math.kent.edu

Given two distinct elements K and K' in $\mathcal{T}_h$, the intersection $\overline{K} \cap \overline{K'}$ is empty, a vertex, or a complete edge with two vertices.

Let V_K be the subspace of local functions whose restrictions to K belong to $H_0^1(K)$ and which are trivially extended throughout Ω,

$$V_K = \left\{ v \in H_0^1(\Omega) \colon v|_K \in H_0^1(K) \text{ and } v|_{\Omega \setminus \overline{K}} = 0 \right\}.$$

Any member function of V_K has a zero trace on the boundary $\partial\Omega$ and on the interface Γ. Let W_Γ be the subspace of trace functions on Γ for all functions in $H_0^1(\Omega)$. Denote V_Γ the subspace of energy-minimizing extensions of trace functions on Γ,

$$V_\Gamma = \left\{ E_\Omega \tau \in H_0^1(\Omega) \colon \tau \in W_\Gamma \right\},$$

where the extension $E_\Omega(\tau)$ solves the minimization problem

$$\inf_{v \in H_0^1(\Omega)} a(v,v) \quad \text{subject to} \quad v|_\Gamma = \tau.$$

The energy-minimizing extension $E_\Omega(\tau)$ satisfies, in the weak sense,

$$\begin{aligned} -\nabla \cdot (\mathbf{A}(\mathbf{x}) \nabla E_\Omega \tau(\mathbf{x})) &= 0 && \text{in } K, \forall K \in \mathcal{T}_h, \\ E_\Omega \tau &= \tau && \text{on } \Gamma, \\ E_\Omega \tau &= 0 && \text{on } \partial\Omega. \end{aligned} \tag{2.3}$$

This property indicates that functions in V_Γ are governed by the underlying partial differential equation. Note that any non-zero member function of V_Γ has a non-zero trace on Γ.

A key result is the orthogonal decomposition

$$H_0^1(\Omega) = \left(\bigoplus_{K \in \mathcal{T}_h} V_K \right) \oplus V_\Gamma. \tag{2.4}$$

The decomposition (2.4) is orthogonal with respect to the inner product $a(\cdot,\cdot)$ because

$$\begin{aligned} a(v,w) &= 0 && \forall v \in V_K, \forall w \in V_{K'}, (K \neq K'), \\ a(v, v_\Gamma) &= 0 && \forall v \in V_K, \forall v_\Gamma \in V_\Gamma. \end{aligned}$$

The former equality follows because the supports of the two functions v and w are disjoint. The latter equality follows by definition of the extension (2.3). Although not often stated in this form, result (2.4) is at the heart of the analysis and development of domain decomposition methods for elliptic partial differential equations [16, 29, 31] and modern component mode synthesis methods [7, 10].

An approximating subspace consistent with the decomposition (2.4) arises from selecting basis functions in the subspaces V_K and V_Γ. To build this approximating subspace, we introduce two different sets of eigenvalue problems. First, we define *fixed-interface* eigenvalue problems: find $(z_{*,K}, \lambda_{*,K}) \in V_K \times \mathbb{R}$ such that

$$a(z_{*,K}, v) = \lambda_{*,K} \left(z_{*,K}, v \right) \quad \forall v \in V_K.$$

Next, for any open edge $e \subset \Gamma$, the edge-based *coupling* eigenvalue problem is: find $(\tau_{*,e}, \lambda_{*,e}) \in H_{00}^{\frac{1}{2}}(e) \times \mathbb{R}$ such that

$$a\left(E_\Omega\left(\tilde{\tau}_{*,e}\right), E_\Omega\left(\tilde{\eta}\right)\right) = \lambda_{*,e} \int_e \tau_{*,e} \eta de \quad \forall \eta \in H_{00}^{\frac{1}{2}}(e),$$

ETNA
Kent State University
http://etna.math.kent.edu

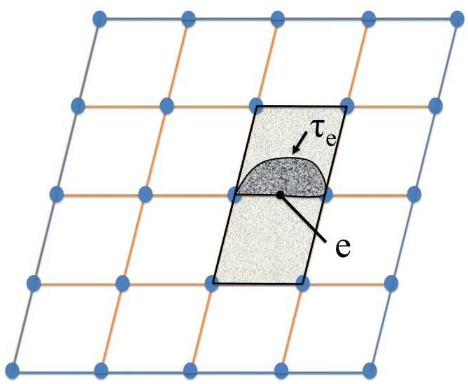

FIG. 2.1. *Example of an edge-bubble eigenfunction along an interior edge* e*.*

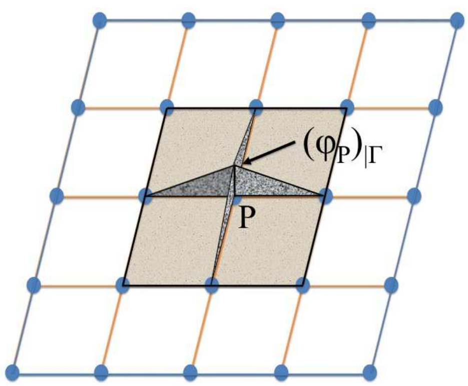

FIG. 2.2. *Trace of* φ_P *along* Γ *for a domain partitioned into 16 elements.*

where $\tilde{\eta}$ denotes the trivial extension of η by 0 on Γ. The eigenvalues $\{\lambda_{i,K}\}_{i=1}^{\infty}$ and $\{\lambda_{i,e}\}_{i=1}^{\infty}$ are assumed to be ordered into nondecreasing sequences. The eigenmodes $z_{*,K}$ and $\tau_{*,e}$ form orthonormal bases for the L^2-inner product on the element K and the edge e, respectively. Figure 2.1 illustrates an example for an eigenfunction τ_e.

To complete the approximating subspace, each *vertex-specific* function φ_P is defined as the harmonic extension satisfying

$$\begin{aligned} -\nabla \cdot (\mathbf{A}(\mathbf{x})\nabla\varphi_P(\mathbf{x})) &= 0 && \text{in } K, \\ \varphi_P &= 0 && \text{on } \partial\Omega, \\ \varphi_P &\neq 0 && \text{on } \Gamma, \\ \varphi_P(P') &= \delta_{P,P'}, \end{aligned}$$

for any element K, where $\delta_{P,P'}$ is the Kronecker delta function. Here φ_P is chosen to be linear on each edge e[1]. On Γ, the trace for φ_P has local support along the boundaries of elements sharing the vertex P. The resulting function φ_P will also have as support the elements sharing the point P. Figure 2.2 illustrates an example of the trace of φ_P.

[1]Efendiev and Hou [15] discuss other choices for φ_P.

ETNA
Kent State University
http://etna.math.kent.edu

The conforming discretization space V_{ACMS}, proposed in [20], is consistent with the orthogonal decomposition (2.4) and is defined as follows:

$$V_{\text{ACMS}} = \left(\bigoplus_{K \in \mathcal{T}_h} \text{span}\left\{ z_{i,K}; 1 \leq i < I_K \right\} \right) \\ \oplus \left[\left(\bigoplus_{P \in \Omega} \text{span}\left\{ \varphi_P \right\} \right) \oplus \left(\bigoplus_{e \subset \Gamma} \text{span}\left\{ E_\Omega\left(\tilde{\tau}_{i,e}\right); 1 \leq i < I_e \right\} \right) \right],$$

where I_K and I_e are positive integers[2]. The letter A in ACMS stands for approximate. Note that the vertices P and the edges e are taken in the interior of Ω. The basis functions have local support and the homogeneous Dirichlet boundary condition is built into V_{ACMS}.

In summary, the conforming finite-dimensional subspace $V_{\text{ACMS}} \subset H_0^1(\Omega)$ exploits the orthogonal decomposition (2.4) for incorporating information from the variational form $a(\cdot, \cdot)$. The subspace V_{ACMS} contains information within elements via the *bubble* eigenfunctions. The functions φ_P and $E_\Omega\left(\tilde{\tau}_{i,e}\right)$ carry information among several and two elements, respectively.

3. Error estimates. The goal of this section is to derive error estimates for the difference of the exact solution u of (2.2) and the approximate solution $u_{\text{ACMS}} \in V_{\text{ACMS}}$ defined by

$$a\left(u_{\text{ACMS}}, v\right) = (f, v) \qquad \forall v \in V_{\text{ACMS}}. \tag{3.1}$$

The orthogonal decomposition (2.4) implies that

$$a\left(u - u_{\text{ACMS}}, u - u_{\text{ACMS}}\right) = a\left(u_B - u_{\text{ACMS},B}, u_B - u_{\text{ACMS},B}\right) \\ + a\left(u_\Gamma - u_{\text{ACMS},\Gamma}, u_\Gamma - u_{\text{ACMS},\Gamma}\right), \tag{3.2}$$

where the solution u satisfies

$$u = u_B + u_\Gamma, \qquad u_B \in \left(\bigoplus_{K \in \mathcal{T}_h} V_K \right) \text{ and } u_\Gamma \in V_\Gamma,$$

and the approximation $u_{\text{ACMS}} \in V_{\text{ACMS}}$ is written as

$$u_{\text{ACMS}} = u_{\text{ACMS},B} + u_{\text{ACMS},\Gamma}, \qquad u_{\text{ACMS},B} \in \left(\bigoplus_{K \in \mathcal{T}_h} V_K \right) \text{ and } u_{\text{ACMS},\Gamma} \in V_\Gamma.$$

The two error terms in (3.2) are treated separately.

LEMMA 3.1. *The components u_B and $u_{\text{ACMS},B}$ satisfy*

$$a\left(u_B - u_{\text{ACMS},B}, u_B - u_{\text{ACMS},B}\right) \leq \sum_{K \in \mathcal{T}_h} \frac{\|f\|^2_{L^2(K)}}{\lambda_{I_K,K}} \leq Ch^2 \sum_{K \in \mathcal{T}_h} \frac{\|f\|^2_{L^2(K)}}{\alpha_{\min,K} I_K}, \tag{3.3}$$

where C is a constant and $\alpha_{\min,K}$ verifies

$$0 < \alpha_{\min,K} \boldsymbol{\xi}^T \boldsymbol{\xi} \leq \boldsymbol{\xi}^T \mathbf{A}(\mathbf{x}) \boldsymbol{\xi} \qquad \forall \mathbf{x} \in K \text{ and } \boldsymbol{\xi} \in \mathbb{R}^2 \setminus \{\mathbf{0}\}. \tag{3.4}$$

[2] When I_K is 1, the subspace span $\left\{ z_{i,K}; 1 \leq i < I_K \right\}$ is equal to $\{0\}$ (the same convention holds for I_e).

Proof. By Galerkin orthogonality, the error satisfies

$$a\left(u_B - u_{\text{ACMS},B}, u_B - u_{\text{ACMS},B}\right) \leq a\left(u_B - w, u_B - w\right) \qquad \forall w \in \left(\bigoplus_{K \in \mathcal{T}_h} \operatorname{span}\left\{z_{i,K}; 1 \leq i < I_K\right\}\right).$$

For every element K, define the projection operator $\mathcal{P}_{I_K}$ as follows

$$\forall v \in L^2(K): \quad \mathcal{P}_{I_K}(v) = \sum_{i=1}^{I_K - 1} \left(\int_K z_{i,K} v\right) z_{i,K}. \tag{3.5}$$

Replacing w by $\mathcal{P}_{I_K}(u_B)$, the projection error for u_B verifies

$$a\left(u_B - \mathcal{P}_{I_K}(u_B), u_B - \mathcal{P}_{I_K}(u_B)\right) = \sum_{K \in \mathcal{T}_h} \int_K \left(\nabla u_B - \nabla \mathcal{P}_{I_K}(u_B)\right)^T \mathbf{A} \left(\nabla u_B - \nabla \mathcal{P}_{I_K}(u_B)\right).$$

On element K, properties of the family of eigenfunctions $(z_{i,K})_{i=1}^{+\infty}$ indicate that

$$\int_K \left(\nabla u_B - \nabla \mathcal{P}_{I_K}(u_B)\right)^T \mathbf{A} \left(\nabla u_B - \nabla \mathcal{P}_{I_K}(u_B)\right) = \sum_{i=I_K}^{+\infty} \lambda_{i,K} \left(\int_K u_B z_{i,K}\right)^2.$$

For every eigenvector $z_{i,K}$, we have

$$\begin{aligned}\int_K u_B z_{i,K} &= \frac{1}{\lambda_{i,K}} \int_K (\nabla u_B)^T \mathbf{A} \nabla z_{i,K} = \frac{1}{\lambda_{i,K}} \int_K \left(-\nabla \cdot (\mathbf{A} \nabla u_B)\right) z_{i,K} \\ &= \frac{1}{\lambda_{i,K}} \int_K f z_{i,K}.\end{aligned}$$

Hence, we get

$$\begin{aligned}&\int_K \left(\nabla u_B - \nabla \mathcal{P}_{I_K}(u_B)\right)^T \mathbf{A} \left(\nabla u_B - \nabla \mathcal{P}_{I_K}(u_B)\right) \\ &= \sum_{i=I_K}^{+\infty} \frac{1}{\lambda_{i,K}} \left(\int_K f z_{i,K}\right)^2 \leq \frac{\|f - \mathcal{P}_{I_K}(f)\|_{L^2(K)}^2}{\lambda_{I_K,K}} \leq \frac{\|f\|_{L^2(K)}^2}{\lambda_{I_K,K}}.\end{aligned}$$

Thus, the projection error $u_B - \mathcal{P}_{I_K}(u_B)$ satisfies

$$a\left(u_B - \mathcal{P}_{I_K}(u_B), u_B - \mathcal{P}_{I_K}(u_B)\right) = \sum_{K \in \mathcal{T}_h} \frac{\|f\|_{L^2(K)}^2}{\lambda_{I_K,K}}.$$

By (3.4), the eigenvalue $\lambda_{i,K}$ is larger than $\alpha_{\min,K}$ times the i-th eigenvalue of the Laplacian on K. By combining the bound of Bourquin on eigenvalues for the Laplacian [9, p. 74] and the shape regularity of the family $(\mathcal{T}_h)_h$, there exists a constant C independent of K and i such that

$$\lambda_{i,K} \geq C \alpha_{\min,K} \frac{i}{h^2}. \tag{3.6}$$

This estimate concludes the proof. ∎

This result uses only the regularity assumption that $-\nabla \cdot (\mathbf{A}\nabla u) = f$ belongs to $L^2(\Omega)$. When f is more regular, a sharper bound for the projection error exists. The lower bound (3.6) is valid for all eigenvalues, while Weyl's formula for eigenvalues is asymptotic; see Bourquin [10, Equation (95)].

Next, the error in V_Γ is estimated.

LEMMA 3.2. *The components u_Γ and $u_{\text{ACMS},\Gamma}$ satisfy*

$$a\left(u_\Gamma - u_{\text{ACMS},\Gamma}, u_\Gamma - u_{\text{ACMS},\Gamma}\right) \le C_{s_0,\sigma,\mathbf{A}} h^{2s_0-3} \sum_{K\in\mathcal{T}_h} \frac{\|u\|^2_{H^{s_0}(K)}}{\min_{e\subset\partial K\cap\Gamma} \lambda_{I_e,e}}, \tag{3.7}$$

when the solution u belongs to $H^{s_0}(\Omega) \cap H^1_0(\Omega)$.

Proof. By Galerkin orthogonality, the error satisfies

$$a\left(u_\Gamma - u_{\text{ACMS},\Gamma}, u_\Gamma - u_{\text{ACMS},\Gamma}\right) \le a\left(u_\Gamma - w, u_\Gamma - w\right) \quad \forall w \in V_\Gamma.$$

Recall that the function u_Γ is equal to $E_\Omega(u|_\Gamma)$. Using the same characterization for w yields

$$a\left(u_\Gamma - w, u_\Gamma - w\right) = \sum_{K\in\mathcal{T}_h} \int_K \left(\nabla E_\Omega(u|_\Gamma - w|_\Gamma)\right)^T \mathbf{A}\nabla E_\Omega(u|_\Gamma - w|_\Gamma).$$

When the restriction $u|_e - w|_e$ belongs to $H^{\frac{1}{2}}_{00}(e)$ for every edge $e \subset \Gamma$, we have on K

$$E_\Omega\left(u|_\Gamma - w|_\Gamma\right) = E_\Omega\left(u|_{\partial K} - w|_{\partial K}\right) = \sum_{e\subset\partial K} E_\Omega\left(\widetilde{u|_e - w|_e}\right),$$

where $\widetilde{u|_e - w|_e}$ is the trivial extension of $(u-w)|_e$ by 0 on Γ. This relation yields

$$\begin{aligned} &a\left(u_\Gamma - w, u_\Gamma - w\right) \\ &\quad = \sum_{K\in\mathcal{T}_h} \int_K \left(\sum_{e\subset\partial K} \nabla E_\Omega\left(\widetilde{u|_e - w|_e}\right)\right)^T \mathbf{A} \left(\sum_{e\subset\partial K} \nabla E_\Omega\left(\widetilde{u|_e - w|_e}\right)\right) \end{aligned}$$

and

$$\begin{aligned} &a\left(u_\Gamma - w, u_\Gamma - w\right) \\ &\quad \le C \sum_{K\in\mathcal{T}_h} \sum_{e\subset\partial K} \int_K \left(\nabla E_\Omega\left(\widetilde{u|_e - w|_e}\right)\right)^T \mathbf{A} \left(\nabla E_\Omega\left(\widetilde{u|_e - w|_e}\right)\right), \end{aligned} \tag{3.8}$$

where the Cauchy-Schwarz inequality has been used. The support of $\widetilde{u|_e - w|_e}$ is included in $\overline{e}$. Its energy-minimizing extension has a local support in $\overline{K}_{e,1} \cup \overline{K}_{e,2}$, where $K_{e,1}$ and $K_{e,2}$ are the two elements whose boundaries share the edge e. Rearranging the terms in (3.8) gives

$$\begin{aligned} &a\left(u_\Gamma - w, u_\Gamma - w\right) \\ &\quad \le C \sum_{e\subset\Gamma} \int_{K_{e,1}\cup K_{e,1}} \left(\nabla E_\Omega\left(\widetilde{u|_e - w|_e}\right)\right)^T \mathbf{A} \left(\nabla E_\Omega\left(\widetilde{u|_e - w|_e}\right)\right). \end{aligned} \tag{3.9}$$

To construct such a function w, we proceed as follows. Let $\mathcal{I}_h$ be the piecewise linear interpolation operator on Γ and define the projection operator Π_{I_e}, for each interior edge e, as follows

$$\forall \eta \in L^2(e): \qquad \Pi_{I_e}(\eta) = \sum_{i=1}^{I_e-1} \left(\int_e \tau_{i,e}\eta\right) \tau_{i,e}.$$

ETNA
Kent State University
http://etna.math.kent.edu

We replace the function w by

$$w = E_\Omega \left(\mathcal{I}_h\left(u_\Gamma\right) + \sum_{e \subset \Gamma} \widetilde{\Pi}_{I_e}\left(u_\Gamma - \mathcal{I}_h\left(u_\Gamma\right)\right) \right) \in V_\Gamma \cap V_{\text{ACMS}},$$

where $\widetilde{\Pi}_{I_e}(\eta)$ is the extension by 0 of $\Pi_{I_e}(\eta)$ on Γ. For this choice of w, we have

$$u|_e - w|_e \in H^{\frac{1}{2}}_{00}(e)$$

for every edge $e \subset \Gamma$.

Assumption 1 indicates that $E_\Omega(u|_\Gamma)$ belongs to $H^{s_0}(\Omega)$. Hence, the restriction $u|_e - \mathcal{I}_h(u)|_e$ is contained in $H^{\frac{1}{2}}_{00}(e) \cap H^1(e)$ for every edge $e \subset \Gamma$. The relations (3.9) and (A.2) yield

$$a\left(u_\Gamma - w, u_\Gamma - w\right) \leq C_{s_0,\sigma,\mathbf{A}} \sum_{e \subset \Gamma} \frac{\left\|u - \mathcal{I}_h\left(u\right)\right\|^2_{H^1(e)}}{\lambda_{I_e,e}}. \tag{3.10}$$

Properties of the interpolation operator $\mathcal{I}_h$ give

$$\left\|u - \mathcal{I}_h\left(u\right)\right\|^2_{H^1(e)} \leq Ch^{2(s_0 - \frac{3}{2})} \left|u\right|^2_{H^{s_0-\frac{1}{2}}(e)} \leq Ch^{2(s_0-\frac{3}{2})} \left\|u\right\|^2_{H^{s_0-\frac{1}{2}}(e)};$$

see Steinbach [30]. Relation (3.10) becomes

$$a\left(u_\Gamma - w, u_\Gamma - w\right) \leq C_{s_0,\sigma,\mathbf{A}} h^{2(s_0-\frac{3}{2})} \sum_{K \in \mathcal{T}_h} \frac{\sum_{e \subset \partial K} \left\|u\right\|^2_{H^{s_0-\frac{1}{2}}(e)}}{\min_{e \subset \partial K \cap \Gamma} \lambda_{I_e,e}}.$$

A theorem of Arnold et al. [2, Theorem 6.1] indicates that we have

$$\sum_{e \subset \partial K} \left\|u\right\|^2_{H^{s_0-\frac{1}{2}}(e)} \leq C \left\|u\right\|^2_{H^{s_0}(K)}$$

because u is continuous on $\overline{\Omega}$ and satisfies the conditions for traces on a polygon. Finally we get

$$a\left(u_\Gamma - w, u_\Gamma - w\right) \leq C_{s_0,\sigma,\mathbf{A}} h^{2s_0-3} \sum_{K \in \mathcal{T}_h} \frac{\left\|u\right\|^2_{H^{s_0}(K)}}{\min_{e \subset \partial K \cap \Gamma} \lambda_{I_e,e}}. \qquad \square$$

To the best of the authors' knowledge, a lower bound on all the *edge-bubble* eigenvalues $\lambda_{*,e}$ is not available. Based on the discussion in Bourquin [9, p. 89] and on egde-related eigenvalues for particular geometries (see, for example, [10, p. 412]), one could expect that

$$\lambda_{l,e} \geq C\alpha_{\min} \frac{l}{h}, \tag{3.11}$$

where the constant C does not depend on e or l. The error (3.7) would become

$$a\left(u_\Gamma - u_{\text{ACMS},\Gamma}, u_\Gamma - u_{\text{ACMS},\Gamma}\right) \leq C_{s_0,\sigma,\mathbf{A}} \frac{h^{2s_0-2}}{\alpha_{\min}} \sum_{K \in \mathcal{T}_h} \frac{\left\|u\right\|^2_{H^{s_0}(K)}}{\min_{e \subset \partial K \cap \Gamma} I_e}, \tag{3.12}$$

providing a rate of h^2 when u belongs to $H^2\left(\Omega\right)$.

REMARK 3.3. The result in Lemma 3.2 does not exhibit an optimal behavior with respect to the edge-based *coupling* eigenvalues when $s_0 > \frac{3}{2}$. Indeed, bounds on the eigendecomposition do not take into account the smoothness of $u_{|\Gamma}$ beyond $H^1(\Gamma)$. Such analysis for the Steklov-Poincaré operator seems difficult to establish.

Combining (3.2) and the previous two lemmas yields the error estimate for u.

PROPOSITION 3.4. *Assume that the solution u of (2.2) belongs to $H_0^1(\Omega) \cap H^{s_0}(\Omega)$, with $s_0 > \frac{3}{2}$. Then the error between the solution u and the approximate solution $u_{\text{ACMS}} \in V_{\text{ACMS}}$ satisfies*

$$a\left(u - u_{\text{ACMS}}, u - u_{\text{ACMS}}\right) \leq \sum_{K \in \mathcal{T}_h} \frac{\|f\|^2_{L^2(K)}}{\lambda_{I_K,K}} + C_{s_0,\sigma,\mathbf{A}} h^{2s_0-3} \sum_{K \in \mathcal{T}_h} \frac{\|u\|^2_{H^{s_0}(K)}}{\min_{e \subset \partial K \cap \Gamma} \lambda_{I_e,e}},$$

where the constant $C_{s_0,\sigma,\mathbf{A}}$ does not depend on u and h.

Note that the approximation u_{ACMS} converges to u even without any *bubble* eigenfunction (i.e., $I_K = 1$). For every element K, the first eigenvalue $\lambda_{1,K}$ verifies $\lambda_{1,K} \geq C\frac{\alpha_{\min}}{h^2}$, which yields

$$a\left(u - u_{\text{ACMS}}, u - u_{\text{ACMS}}\right) \leq C\frac{h^2}{\alpha_{\min}} \|f\|^2_{L^2(\Omega)} + C_{s_0,\sigma,\mathbf{A}} h^{2s_0-3} \sum_{K \in \mathcal{T}_h} \frac{\|u\|^2_{H^{s_0}(K)}}{\min_{e \subset \partial K \cap \Gamma} \lambda_{I_e,e}}.$$

When $I_K = I_e = 1$, the approximation u_{ACMS} still converges to u thanks to the *vertex-specific* functions. This particular case was proved in [12, 22].

REMARK 3.5. The error estimates in Proposition 3.4 are closely related to the pioneering work of Bourquin [8, 9, 10] on component mode synthesis. The main difference lies in the way the information is transferred among elements. Bourquin uses eigenmodes on Γ for the Steklov-Poincaré operator. Here the *vertex-specific* functions φ_P and the *edge-bubble* eigenfunctions carry information among elements and have local support.

The choice of basis functions in V_{ACMS} determine the efficiency of the discretization method. The number of eigenfunctions cannot be known in advance and should be estimated adaptively during the computations. The following proposition introduces an a posteriori error indicator that could guide how to select the number of *bubble* eigenfunctions and *edge-bubble* eigenfunctions.

PROPOSITION 3.6. *The error between u and u_{ACMS} satisfies*

$$\sqrt{a\left(u - u_{\text{ACMS}}, u - u_{\text{ACMS}}\right)} \leq C_{\varepsilon,\sigma,\mathbf{A}} \left\{ \sum_{K \in \mathcal{T}_h} \frac{\|f - \mathcal{P}_{I_K}(f)\|^2_{L^2(K)}}{\lambda_{I_K,K}} + h^{2\varepsilon} \sum_{K \in \mathcal{T}_h} \|f - \mathcal{P}_{I_K}(f)\|^2_{L^2(K)} \left(\sum_{e \subset \partial K \cap \Gamma} \frac{1}{\lambda^{2-2\varepsilon}_{I_e,e}} \right) + h^{2\varepsilon} \sum_{e \subset \Gamma} \frac{\left\| J_e\left(\boldsymbol{\nu}_e^T \mathbf{A} \nabla u_{\text{ACMS}}\right)\right\|^2_{L^2(e)}}{\lambda^{1-2\varepsilon}_{I_e,e}} \right\}^{\frac{1}{2}}, \tag{3.13}$$

ETNA
Kent State University
http://etna.math.kent.edu

where $\varepsilon > 0$ *and* $J_e(\psi)$ *denotes the jump of a given function* ψ *across the edge* e *in the direction of the unit normal vector* $\boldsymbol{\nu}_e$. *The constant* $C_{\varepsilon,\sigma,\mathbf{A}}$ *depends on* ε, σ, *and the coefficient matrix* $\mathbf{A}$.

The proof is given in Appendix B. Bound (3.13) indicates that the right hand side defines an a posteriori error indicator. This error indicator is reliable, i.e., the error is bounded from above by multiples of the indicator. Proving the effectivity of the error indicator remains an open question.

REMARK 3.7. In practice, the basis functions are computed numerically by introducing a nested finer grid. The selection of this nested finer grid impacts both the accuracy and the complexity of the algorithm. Finding error estimates and a posteriori error indicators for such a two-grid scheme remains an open problem that is beyond the scope of this paper; see [11] and [19] for a recent study applied to the multiscale finite element method. A complexity comparison between a two-grid scheme and the standard application of the finite element method would require a specific study with careful numerical experiments. However, to estimate the merit of the two-grid scheme over the standard application of the finite element method, flop count expressions are briefly discussed in the same style as the comparison of Hou and Wu [21, Section 4.2].

If $\frac{h}{M}$ denotes the fine mesh size, then the fine grid yields $\mathcal{O}\left(M^2 h^{-2}\right)$ degrees of freedom. The computational complexity associated with the standard application of the finite element method over the fine grid is dominated by the operation count for solving the linear system,

$$\mathcal{O}\left((M^2 h^{-2})^{\alpha}\right) = \mathcal{O}(M^{2\alpha} h^{-2\alpha}),$$

where $\alpha \in [1, 3]$ depends on the specific linear solver used[3]. The complexity for the two-grid scheme based on component mode synthesis is

$$\mathcal{O}(h^{-2\alpha}) + \max\left[\mathcal{O}(M^{2\alpha} h^{-2}), \mathcal{O}(M^6 h^{-2}), \mathcal{O}(M^{2\alpha+1} h^{-2})\right],$$

where $\mathcal{O}(h^{-2\alpha})$ is the cost of solving the algebraic equation (3.1). The other term estimates the cost for computing the basis functions φ_P, $z_{*,K}$, and $E_\Omega(\tilde{\tau}_{*,e})$, respectively. The complexity for computing all the *vertex-specific* functions φ_P is $\mathcal{O}(M^{2\alpha} h^{-2})$. The *bubble* eigenfunctions $z_{*,K}$ require, at most, $\mathcal{O}(M^6 h^{-2})$ operations. Note that this cost is an overestimate because it does not exploit the fact that only $I_K \ll M^2$ eigenmodes of a sparse pencil are needed. $\mathcal{O}(M^{2\alpha+1} h^{-2})$ estimates the complexity for computing the *edge-bubble* eigenfunctions $E_\Omega(\tilde{\tau}_{*,e})$.

When $\alpha = 1$, the two-grid scheme is not attractive from an operation count point of view. However, solvers with $\alpha = 1$ are not common or available for a general coefficient matrix $\mathbf{A}$. As soon as $\alpha > 1$, a two-grid scheme has some merit, especially when M is smaller than $h^{-\frac{1}{3}}$.

4. Numerical experiments. In this section, numerical experiments illustrate the sharpness of the previous bounds at academic examples. When the exact solution is not known explicitly, the energy,

$$\mathcal{E}(v) = \frac{1}{2} \int_\Omega (\nabla v(\mathbf{x}))^T \mathbf{A}(\mathbf{x}) \nabla v(\mathbf{x})\, d\mathbf{x} - \int_\Omega f(\mathbf{x})\, v(\mathbf{x})\, d\mathbf{x},$$

represents an intrinsic metric for comparing the quality of approximations to the exact solution. Computing the difference between the energy of the computed solution and the energy

[3] For a finite element discretization in two dimensions, a sparse solver is usually characterized by $\alpha = \frac{3}{2}$; see, for example, Heath [18, Table 11.4].

ETNA
Kent State University
http://etna.math.kent.edu

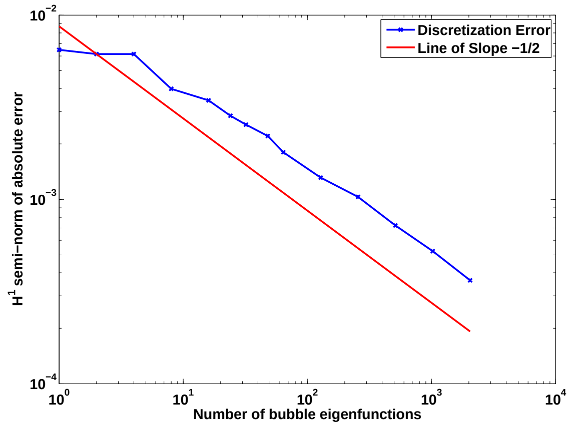

FIG. 4.1. *Convergence curve for solution* (4.1) *with* $\alpha = 1.51$ *and* $h = 1$ *(squared domain).*

of the exact solution, $\mathcal{E}^* = \mathcal{E}(u)$, is equivalent to computing the norm of the error for the energy inner product,

$$\mathcal{E}(v) - \mathcal{E}^* = \frac{a(u-v, u-v)}{2}.$$

The minimum energy $\mathcal{E}^*$ is obtained by extrapolating energies for finite element solutions on fine meshes.

4.1. Convergence towards a smooth solution. In this section, consider the problem

$$-\Delta u = f \quad \text{in } \Omega = [0,1] \times [0,1], \quad u = 0 \quad \text{on } \partial\Omega,$$

where the domain $[0,1] \times [0,1]$ is partitioned by square elements.

First, the function f is chosen so that the exact solution is

$$u(x,y) = \left(\left(x - x^2\right)\left(y - y^2\right)\right)^{\alpha}, \tag{4.1}$$

where $\alpha > \frac{3}{2}$. Figure 4.1 illustrates the convergence when *only one* element is used and the number of *bubble* eigenfunctions is increased. When $\alpha = 1.51 \approx \frac{3}{2} + \varepsilon$, the right hand side f belongs to $L^2(\Omega)$. The convergence curve exhibits a decrease proportional to $\frac{1}{\sqrt{\lambda_I}}$, which is predicted by the bound (3.3).

When $f = 1$, the right hand side now belongs to $H^{\frac{1}{2}}(\Omega)$. In Figure 4.2, the convergence, when *only one* element is used and the number of *bubble* eigenfunctions is increased, exhibits a higher convergence rate, which is described by the projection error of f,

$$\frac{\|f - \mathcal{P}_I f\|_{L^2(\Omega)}}{\sqrt{\lambda_I}} \leq \frac{\|f\|_{L^2(\Omega)}}{\sqrt{\lambda_I}}.$$

Keeping $f = 1$ and using only one *bubble* eigenfunction and one *edge-bubble* eigenfunction, Figure 4.3 illustrates the convergence when the number of elements is increased. As expected, the convergence curve exhibits a decrease proportional to the mesh size h.

The next study keeps $f = 1$ and uses $h = \frac{1}{2}$ and 4096 *bubble* eigenfunctions for every element. Figure 4.4 illustrates the convergence when the number of *edge-bubble* eigenfunctions is increased. The convergence curve exhibits a plateau because the number of bubble

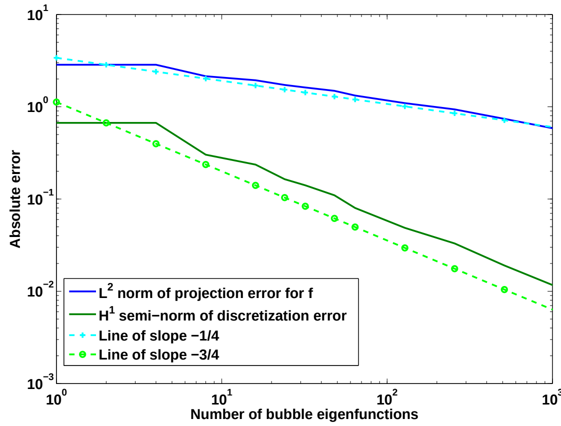

FIG. 4.2. *Convergence curve when $f = 1$ and $h = 1$ (squared domain).*

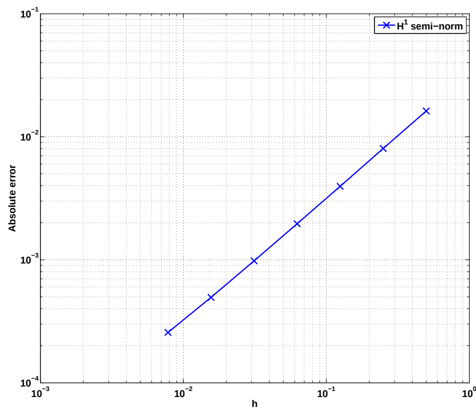

FIG. 4.3. *Convergence curve when $f = 1$ (squared domain).*

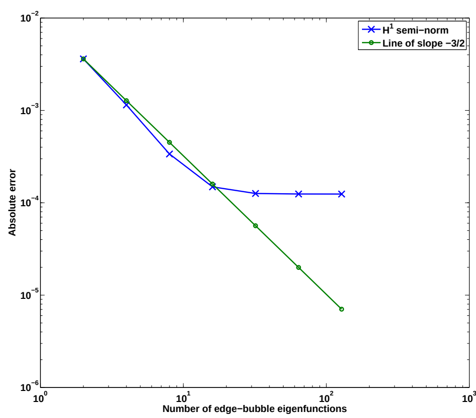

FIG. 4.4. *Convergence curve when $f = 1$, $h = \frac{1}{2}$, and 4096 bubble eigenfunctions are used (squared domain).*

ETNA
Kent State University
http://etna.math.kent.edu

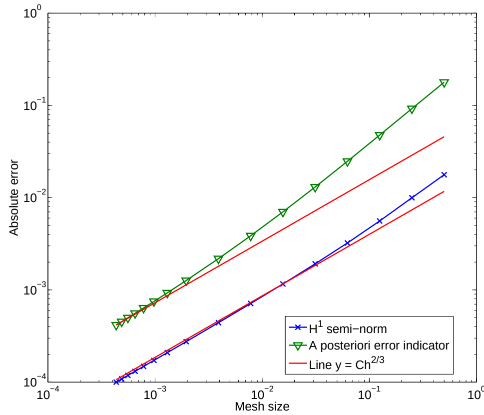

FIG. 4.5. *Convergence curve for a fixed number of bubble and edge-bubble eigenfunctions (L-shaped domain, $f = 1$).*

eigenfunctions is fixed. Before reaching this asymptote, the curve decreases like $I_e^{-\frac{3}{2}}$. This rate is higher than the prediction in (3.12). Bourquin [9, p. 45] indicates that, for smooth functions, a superconvergence phenomenon is expected with the precise rate $I_e^{-\frac{3}{2}}$.

4.2. Problem on a L-shaped domain. In this section, consider the problem

$$-\Delta u = 1 \quad \text{in } \Omega = ([0,1]\times[0,1]) \setminus \left(\left[\frac{1}{2},1\right] \times \left[\frac{1}{2},1\right]\right), \quad u = 0 \quad \text{on } \partial\Omega,$$

where the domain Ω is partitioned by square elements. The exact solution belongs to $H^{\frac{5}{3}}(\Omega) \cap H_0^1(\Omega)$. For this problem, the approximate value for $\mathcal{E}^*$ is

$$\mathcal{E}^* = -6.689868958058575 \times 10^{-3}.$$

Proposition 3.4, bound (3.6), and conjecture (3.11) indicate that the error is bounded as follows

$$a\left(u - u_{\text{ACMS}}, u - u_{\text{ACMS}}\right) \leq C \frac{h^2}{\max_K I_K} \left\|f\right\|_{L^2(\Omega)}^2 + C \frac{h^{\frac{4}{3}}}{\max_e I_e} \left\|u\right\|_{H^{\frac{5}{3}}(\Omega)}^2. \tag{4.2}$$

The following experiments illustrate the sharpness of this result.

Using only one *bubble* eigenfunction and one *edge-bubble* eigenfunction, Figure 4.5 illustrates the convergence when the number of elements is increased. As expected, the convergence curve exhibits a decrease proportional to $h^{\frac{2}{3}}$. The a posteriori error indicator (3.13) (with $\varepsilon = 0$) decreases also proportionally to $h^{\frac{2}{3}}$. The ratio between the error indicator and the semi-norm varies between 4 and 10.

Next, only one *bubble* eigenfunction is used while the mesh size h is decreased. The number of *edge-bubble* eigenfunctions is set to the integer part of $\frac{1}{h}$. Figure 4.6 illustrates the convergence when the number of elements is increased. Since $\max_e I_e = \mathcal{O}(\frac{1}{h})$, bound (4.2) suggests a convergence rate of h, which is matched by the numerical experiment. The plot confirms that the impact of *bubble* eigenfunctions depends only on the regularity of the right hand side f.

ETNA
Kent State University
http://etna.math.kent.edu

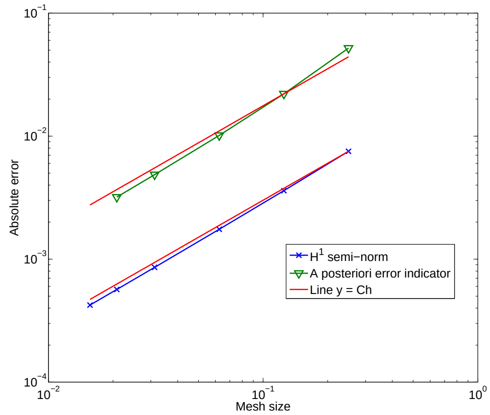

FIG. 4.6. *Convergence curve when $f = 1$ for a fixed number of bubble eigenfunctions (L-shaped domain).*

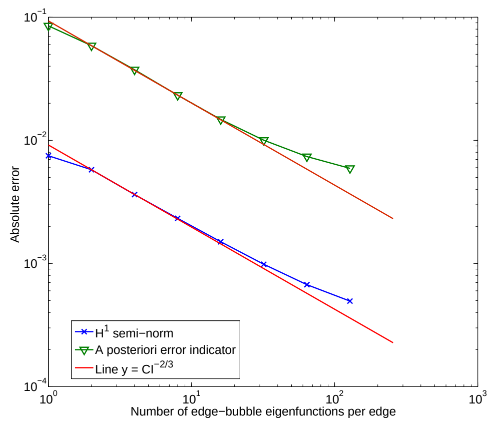

FIG. 4.7. *Convergence curve for a varying number of edge-bubble eigenfunctions (L-shaped domain, $f = 1$, $h = \frac{1}{4}$, $I_K = 256$).*

Finally, in the next experiment, the number of *edge-bubble* eigenfunctions is varied while the mesh size h is set to $\frac{1}{4}$ and the number of *bubble* eigenfunctions to 256. Figure 4.7 illustrates the convergence when the number of *edge-bubble* eigenfunctions is uniformly increased. The semi-norm of the error and the a posteriori error indicator decrease proportionally to $I_e^{-\frac{2}{3}}$ before reaching a plateau set by the constant number of *bubble* eigenfunctions. Bound (4.2) suggests only a decrease proportional to $I_e^{-\frac{1}{2}}$. This discrepancy is due to relation (A.2) which does not exploit smoothness beyond $H^1(\Gamma)$.

4.3. Problem with varying coefficient. Finally, consider the problem

$$
\begin{aligned}
-\nabla\left(c\left(\mathbf{x}\right)\nabla u\left(\mathbf{x}\right)\right) &= -1 \qquad &&\text{in } \Omega = [0,1]\times[0,1]\,,\\
u &= 0 &&\text{on } \partial\Omega,
\end{aligned}
\tag{4.3}
$$

ETNA
Kent State University
http://etna.math.kent.edu

TABLE 4.1
Error evolution for problem (4.3) as the mesh size h is reduced.

Mesh size	$\mathcal{E}(v) - \mathcal{E}^*$	η_{int}	η_{edge}
$h = \frac{1}{4}$	6.81×10^{-2}	1.80×10^{-1}	1.8×10^{-3}
$h = \frac{1}{8}$	2.04×10^{-2}	4.24×10^{-2}	3.6×10^{-4}
$h = \frac{1}{16}$	6.94×10^{-3}	1.31×10^{-2}	6.34×10^{-5}
$h = \frac{1}{32}$	1.35×10^{-3}	3.58×10^{-3}	6.98×10^{-6}

where the coefficient c is

$$c(x, y) = \frac{2 + 1.8 \sin\left(\frac{2\pi x}{\varepsilon}\right)}{2 + 1.8 \cos\left(\frac{2\pi y}{\varepsilon}\right)} + \frac{2 + \sin\left(\frac{2\pi y}{\varepsilon}\right)}{2 + 1.8 \sin\left(\frac{2\pi x}{\varepsilon}\right)}$$

with $\varepsilon = \frac{1}{8}$. The domain Ω is partitioned by square elements. This problem was initially studied in [21]. The exact solution belongs to $H^2(\Omega) \cap H_0^1(\Omega)$. For this problem, the approximate value for $\mathcal{E}^*$ is

$$\mathcal{E}^* = -4.826726636113407 \times 10^{-3}.$$

The objective of this subsection is to assess the quality of the error indicator in Proposition 3.6. Denote

$$\eta_{int} = \sum_{K \in \mathcal{T}_h} \frac{\|f - \mathcal{P}_{I_K}(f)\|^2_{L^2(K)}}{\lambda_{I_K, K}}$$

and

$$\eta_{edge} = \sum_{K \in \mathcal{T}_h} \|f - \mathcal{P}_{I_K}(f)\|^2_{L^2(K)} \left(\sum_{e \subset \partial K \cap \Gamma} \frac{1}{\lambda^2_{I_e, e}} \right) + \sum_{e \subset \Gamma} \frac{\left\| J_e\left(\boldsymbol{\nu}_e^T \mathbf{A} \nabla u_{\text{ACMS}}\right) \right\|^2_{L^2(e)}}{\lambda_{I_e, e}}.$$

Table 4.1 describes the reduction of errors and error indicators as the mesh size is refined. One *edge-bubble* eigenfunction for each edge and no *bubble* eigenfunctions are used. The energy differences and the indicator η_{int} exhibit a reduction proportional to h^2. As can be seen in Figure 4.4, a superconvergence phenomenon for the edge part of errors is possible; see Bourquin [9, p. 45]. Here, the edge indicator η_{edge} is decreasing slightly faster than h^3 for this range of mesh sizes.

Table 4.2 illustrates the same information when the number of *edge-bubble* eigenfunctions is uniformly increased. The mesh size is set to $h = \frac{1}{8}$ and no *bubble* eigenfunction is used. For this setup, the energy differences reach a plateau while the edge indicator η_{edge} is decreasing slightly faster than $(\max_e I_e)^{-1}$, the prediction in (3.12).

5. Conclusion. This paper derives a priori error estimates for a special finite element discretization based on component mode synthesis. The a priori error bounds state the explicit dependency of constants with respect to the mesh size and the first neglected eigenvalues. A residual-based a posteriori error indicator is also presented. Numerical experiments illustrate that the error indicator is reliable.

Such indicator could guide the adaptive selection for the number of *bubble* and *edge-bubble* eigenfunctions. In practice, the basis functions and eigenfunctions used in this special finite element method are computed numerically by introducing a nested finer grid. To enhance the practicality of these special finite elements, future works will study error estimates and a posteriori error indicators for the resulting two-grid scheme.

ETNA
Kent State University
http://etna.math.kent.edu

TABLE 4.2
Error evolution for problem (4.3) as the number of edge-bubble eigenfunctions is increased and $h = \frac{1}{8}$.

Edge-bubble eigenfunctions	$\mathcal{E}(v) - \mathcal{E}^*$	η_{int}	η_{edge}
1	2.04×10^{-2}	4.24×10^{-2}	3.65×10^{-4}
2	1.81×10^{-2}	4.24×10^{-2}	1.69×10^{-4}
4	1.62×10^{-2}	4.24×10^{-2}	5.25×10^{-5}
8	1.59×10^{-2}	4.24×10^{-2}	1.63×10^{-5}

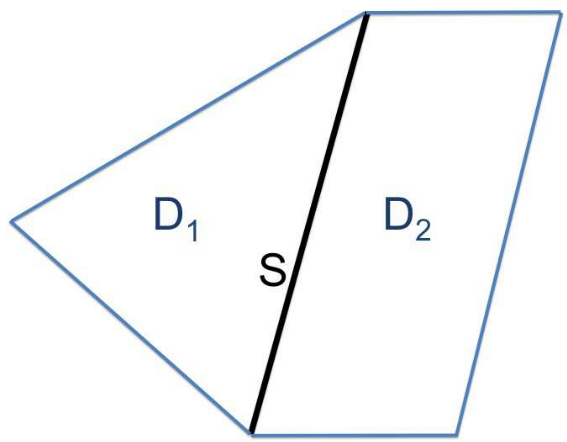

FIG. A.1. *Example of domain D.*

Acknowledgments. U. Hetmaniuk acknowledges the partial support by the National Science Foundation under grant DMS-0914876.

Appendix A. Review of properties of the Steklov-Poincaré operator.

In this section, properties of the Steklov-Poincaré operator are compiled. Further details and references are included in Bourquin [10] and Khoromskij and Wittum [25].

Consider a bounded polygonal domain $D \subset \mathbb{R}^2$ partitioned into two regions, $\overline{D} = \overline{D}_1 \cup \overline{D}_2$. The subdomains D_1 and D_2 are bounded convex polygons with straight edges. The interface $S = \overline{D}_1 \cap \overline{D}_2$ is illustrated in Figure A.1.

For any $\tau \in H_{00}^{\frac{1}{2}}(S)$, the energy-minimizing extension $E_1(\tau) \in H^1(D_1)$ is defined as the unique solution to the problem

$$-\nabla \cdot (\mathbf{A} \nabla E_1(\tau)) = 0 \text{ in } D_1, \quad E_1(\tau) = \tau \text{ on } S, \quad E_1(\tau) = 0 \text{ on } \partial D_1 \cap \partial D.$$

The energy-minimizing $E_2(\tau) \in H^1(D_2)$ is defined similarly in D_2. The matrix $\mathbf{A}$ is uniformly symmetric positive definite on D as described by (2.1).

Introduce the symmetric bilinear form

$$b(\tau, \eta) = \int_{D_1} \nabla E_1(\tau)^T \mathbf{A} \nabla E_1(\eta) + \int_{D_2} \nabla E_2(\tau)^T \mathbf{A} \nabla E_2(\eta),$$

for any function τ and η in $H_{00}^{\frac{1}{2}}(S)$. The continuity and coerciveness of b are consequences of the continuity of the energy-minimizing extension, of the trace operator on S, and of

ETNA
Kent State University
http://etna.math.kent.edu

properties of $\mathbf{A}$. Given that the injection of $H_{00}^{\frac{1}{2}}(S)$ into $L^2(S)$ is compact (see Bourquin [10, p. 390–391]), there exists a self-adjoint unbounded linear operator B on $L^2(S)$ with compact inverse such that

$$b(\tau,\eta) = \int_S (B\tau)\,\eta, \quad \forall \eta \in L^2(S)$$

and for any arbitrary τ in the domain of the operator B,

$$\mathcal{D}(B) = \left\{ \tau \in H_{00}^{\frac{1}{2}}(S)\,;\; B\tau = \boldsymbol{\nu}_1^T \mathbf{A}\nabla E_1(\tau) + \boldsymbol{\nu}_2^T \mathbf{A}\nabla E_2(\tau) \in L^2(S) \right\},$$

where $\boldsymbol{\nu}_1$, respectively $\boldsymbol{\nu}_2$, is the unit outer normal vector to ∂D_1, respectively ∂D_2. Note that the operator B can be decomposed as follows

$$B\tau = B_1\tau + B_2\tau \quad \text{with } B_1\tau = \boldsymbol{\nu}_1^T \mathbf{A}\nabla E_1(\tau) \text{ and } B_2\tau = \boldsymbol{\nu}_2^T \mathbf{A}\nabla E_2(\tau)$$

for any element τ in $\mathcal{D}(B)$.

When η belongs to $H_{00}^{\frac{1}{2}}(S) \cap H^1(S)$, the compatibility conditions for traces on a polygon [2, Theorem 6.1] indicate that η satisfies

$$\tilde{\eta}|_{\partial D_1} \in H^1(\partial D_1) \quad \text{and} \quad \tilde{\eta}|_{\partial D_2} \in H^1(\partial D_2).$$

Then we have

$$\text{(A.1)} \qquad \begin{aligned} \|B\eta\|_{L^2(S)} &\le \|B_1\tilde{\eta}\|_{L^2(\partial D_1)} + \|B_2\tilde{\eta}\|_{L^2(\partial D_2)} \\ &\le C_{\mathbf{A}}\,\|\tilde{\eta}\|_{H^1(\partial D_1)} + C_{\mathbf{A}}\,\|\tilde{\eta}\|_{H^1(\partial D_2)} \le C_{\mathbf{A}}\,\|\eta\|_{H^1(S)}, \end{aligned}$$

where $C_{\mathbf{A}}$ denotes a generic constant that may depend on the coefficient matrix $\mathbf{A}$. The constant $C_{\mathbf{A}}$ does not depend on the length of S or on the diameter of D; see Nečas [27, Theorem 1] for the bound between $\|B_k\tilde{\eta}\|_{L^2(\partial D_k)}$ and $\|\tilde{\eta}\|_{H^1(\partial D_k)}$, where $k = 1, 2$.

Spectral decomposition. Spectral theory yields a family $(\phi_n)_{n=1}^{+\infty}$ forming an orthogonal basis of $H_{00}^{\frac{1}{2}}(S)$ and $L^2(S)$ and a sequence of real numbers $(\theta_n)_{n=1}^{+\infty}$ such that

$$b(\phi_n,\eta) = \theta_n \int_S \phi_n \eta, \qquad \forall \eta \in H_{00}^{\frac{1}{2}}(S),$$

and

$$\int_S \phi_n^2 = 1 \qquad \text{and} \qquad 0 < \theta_1 \le \theta_2 \le \cdots.$$

The eigenfunctions also satisfy $B\phi_n = \theta_n\phi_n$; see Bourquin [10, p. 392].

For $\eta \in L^2(S)$, define the projection

$$\Pi_L(\eta) = \sum_{n=1}^{L-1} \left(\int_S \eta\phi_n \right) \phi_n.$$

When $B\eta$ belongs to $L^2(S)$, we write

$$\int_S \eta\phi_n = \frac{1}{\theta_n}\int_S \eta\,(B\phi_n) = \frac{1}{\theta_n}\int_S (B\eta)\,\phi_n.$$

ETNA
Kent State University
http://etna.math.kent.edu

For $\eta \in H^{\frac{1}{2}}_{00}(S)$ with $B\eta \in L^2(S)$, it holds that

$$b\left(\eta - \Pi_L(\eta), \eta - \Pi_L(\eta)\right) = \sum_{n=L}^{+\infty} \theta_n \left(\int_S \eta \phi_n\right)^2 = \sum_{n=L}^{+\infty} \frac{1}{\theta_n} \left(\int_S (B\eta)\,\phi_n\right)^2$$
$$\leq \frac{1}{\theta_L} \left\| B\eta - \Pi_L(B\eta) \right\|^2_{L^2(S)} \leq \frac{1}{\theta_L} \left\| B\eta \right\|^2_{L^2(S)}.$$

In particular, when $\eta \in H^{\frac{1}{2}}_{00}(S) \cap H^1(S)$, relation (A.1) implies that $B\eta$ belongs to $L^2(S)$. In this case, the projection error satisfies

$$b\left(\eta - \Pi_L(\eta), \eta - \Pi_L(\eta)\right) \leq \frac{C_{\mathbf{A}}}{\theta_L} \left\|\eta\right\|^2_{H^1(S)}. \tag{A.2}$$

Bounds in dual spaces will also be needed. For $\eta \in H^{\frac{1}{2}}_{00}(S)$, we write

$$\left\|\eta - \Pi_L(\eta)\right\|^2_{L^2(S)} = \sum_{n=L}^{+\infty} \left(\int_S \eta\phi_n\right)^2 = \sum_{n=L}^{+\infty} \frac{1}{\theta_n^{2s}} \theta_n^{2s} \left(\int_S \eta\phi_n\right)^2$$
$$\leq \frac{1}{\theta_L^{2s}} \sum_{n=L}^{+\infty} \theta_n^{2s} \left(\int_S \eta\phi_n\right)^2$$

for $0 \leq s < \frac{1}{2}$. Using the equivalence between the norms

$$\sqrt{\sum_{n=1}^{+\infty} (1+\theta_n^{2s}) \left(\int_S \eta\phi_n\right)^2} \quad \text{and} \quad \|\eta\|_{H^s(S)} \quad \text{for } 0 \leq s < \frac{1}{2}$$

(see, for example, Khoromskij and Wittum [25, Section 1.7]), we obtain

$$\left\|\eta - \Pi_L(\eta)\right\|^2_{L^2(S)} \leq \frac{C_{s,\mathbf{A}}}{\theta_L^s} \|\eta\|^2_{H^s(S)} \tag{A.3}$$

for $0 < s < \frac{1}{2}$, where $C_{s,\mathbf{A}}$ does not depend on the length of S.

After continuously extending the projection Π_L to $H^{-\frac{1}{2}}(S) = \left(H^{\frac{1}{2}}_{00}(S)\right)'$, similar estimates hold in $H^{-\frac{1}{2}}(S)$,

$$\left\|\eta - \Pi_L(\eta)\right\|^2_{H^{-\frac{1}{2}}(S)} \leq \frac{1}{\theta_L} \left\|\eta - \Pi_L(\eta)\right\|^2_{L^2(S)} \leq \frac{C_{s,\mathbf{A}}}{\theta_L^{1+2s}} \|\eta\|^2_{H^s(S)} \tag{A.4}$$

for $0 \leq s < \frac{1}{2}$, where $C_{s,\mathbf{A}}$ does not depend on the length of S.

Appendix B. Proof of Proposition 3.6.

Proof. Recall that the exact solution u satisfies

$$a(u,v) = \int_\Omega fv, \quad \forall v \in H^1_0(\Omega)$$

and that $\mathcal{P}_{I_K}$ is the projection operator defined by (3.5). The function f can be decomposed as follows

$$f = \sum_{K\in\mathcal{T}_h} \mathcal{P}_{I_K}(f) + \sum_{K\in\mathcal{T}_h} \left[f - \mathcal{P}_{I_K}(f)\right]$$

ETNA
Kent State University
http://etna.math.kent.edu

such that

$$\begin{aligned}\int_\Omega fv &= \sum_{K\in\mathcal{T}_h}\int_K \mathcal{P}_{I_K}(f)\,v + \sum_{K\in\mathcal{T}_h}\int_K \left[f-\mathcal{P}_{I_K}(f)\right]v \\ &= \sum_{K\in\mathcal{T}_h}\int_K \mathcal{P}_{I_K}(f)\,v_{B,K} + \sum_{K\in\mathcal{T}_h}\int_K \mathcal{P}_{I_K}(f)\,v_\Gamma \\ &\quad + \sum_{K\in\mathcal{T}_h}\int_K \left[f-\mathcal{P}_{I_K}(f)\right]v_{B,K} + \sum_{K\in\mathcal{T}_h}\int_K \left[f-\mathcal{P}_{I_K}(f)\right]v_\Gamma\,,\end{aligned}$$

where the decomposition

$$v = \sum_{K\in\mathcal{T}_h} v_{B,K} + v_\Gamma$$

has been used. The orthogonality of eigenfunctions $z_{*,K}$ yields

$$\begin{aligned}\int_\Omega fv = &\sum_{K\in\mathcal{T}_h}\int_K \mathcal{P}_{I_K}(f)\,\mathcal{P}_{I_K}(v_{B,K}) + \sum_{K\in\mathcal{T}_h}\int_K \mathcal{P}_{I_K}(f)\,v_\Gamma \\ &+ \sum_{K\in\mathcal{T}_h}\int_K \left[f-\mathcal{P}_{I_K}(f)\right]\left[v_{B,K}-\mathcal{P}_{I_K}(v_{B,K})\right] + \sum_{K\in\mathcal{T}_h}\int_K \left[f-\mathcal{P}_{I_K}(f)\right]v_\Gamma\,.\end{aligned}$$

At the same time, the approximate solution $u_{\text{ACMS}} \in V_{\text{ACMS}}$ satisfies

$$a(u_{\text{ACMS}}, v) = \sum_{K\in\mathcal{T}_h}\int_K \left(\nabla u_{\text{ACMS},B}\right)^T \mathbf{A}\nabla\mathcal{P}_{I_K}(v_{B,K}) + \int_\Omega \left(\nabla u_{\text{ACMS},\Gamma}\right)^T \mathbf{A}\nabla v_\Gamma.$$

Integration by parts of the second term over every element K gives

$$\begin{aligned}a(u_{\text{ACMS}}, v) = &\sum_{K\in\mathcal{T}_h}\int_K \left(\nabla u_{\text{ACMS},B}\right)^T \mathbf{A}\nabla\mathcal{P}_{I_K}(v_{B,K}) \\ &+ \sum_{K\in\mathcal{T}_h}\sum_{e\subset\partial K}\int_e \left(\boldsymbol{\nu}_e^T\mathbf{A}\nabla u_{\text{ACMS},\Gamma}\right)v_\Gamma.\end{aligned}$$

Combining all the previous relations, we have

$$\begin{aligned}a(u-u_{\text{ACMS}}, v) = &\sum_{K\in\mathcal{T}_h}\int_K \left[f-\mathcal{P}_{I_K}(f)\right]\left[v_{B,K}-\mathcal{P}_{I_K}(v_{B,K})\right] \\ &+ \sum_{K\in\mathcal{T}_h}\int_K \mathcal{P}_{I_K}(f)\,v_\Gamma + \sum_{K\in\mathcal{T}_h}\int_K \left[f-\mathcal{P}_{I_K}(f)\right]v_\Gamma \\ &+ \sum_{K\in\mathcal{T}_h}\int_K \mathcal{P}_{I_K}(f)\,\mathcal{P}_{I_K}(v_{B,K}) - \sum_{K\in\mathcal{T}_h}\int_K \left(\nabla u_{\text{ACMS},B}\right)^T \mathbf{A}\nabla\mathcal{P}_{I_K}(v_{B,K}) \\ &- \sum_{K\in\mathcal{T}_h}\sum_{e\subset\partial K}\int_e \left(\boldsymbol{\nu}_e^T\mathbf{A}\nabla u_{\text{ACMS},\Gamma}\right)v_\Gamma.\end{aligned} \tag{B.1}$$

On every element K, the bubble function $u_{\text{ACMS},B}$ satisfies

$$-\nabla\cdot\left(\mathbf{A}\nabla u_{\text{ACMS},B}\right) = \mathcal{P}_{I_K}(f)\,.$$

ETNA
Kent State University
http://etna.math.kent.edu

Hence, we get

$$\int_K \left(\nabla u_{\text{ACMS},B}\right)^T \mathbf{A} \nabla \mathcal{P}_{I_K}\left(v_{B,K}\right) = \int_K \mathcal{P}_{I_K}\left(f\right) \mathcal{P}_{I_K}\left(v_{B,K}\right)$$

and

$$\begin{aligned}\int_K \mathcal{P}_{I_K}\left(f\right) v_\Gamma &= -\int_K \nabla \cdot \left(\mathbf{A} \nabla u_{\text{ACMS},B}\right) v_\Gamma \\ &= \int_K \left(\nabla u_{AMCS,B}\right)^T \mathbf{A} \nabla v_\Gamma - \sum_{e \subset \partial K} \int_e \left(\boldsymbol{\nu}_e^T \mathbf{A} \nabla u_{\text{ACMS},B}\right) v_\Gamma \\ &= -\sum_{e \subset \partial K} \int_e \left(\boldsymbol{\nu}_e^T \mathbf{A} \nabla u_{\text{ACMS},B}\right) v_\Gamma\end{aligned} \tag{B.2}$$

by orthogonality. Equations (B.1) and (B.2) yield

$$\begin{aligned}a\left(u - u_{\text{ACMS}}, v\right) = &\sum_{K \in \mathcal{T}_h} \int_K \left[f - \mathcal{P}_{I_K}\left(f\right)\right]\left[v_{B,K} - \mathcal{P}_{I_K}\left(v_{B,K}\right)\right] \\ &+ \sum_{K \in \mathcal{T}_h} \int_K \left[f - \mathcal{P}_{I_K}\left(f\right)\right] v_\Gamma \\ &- \sum_{K \in \mathcal{T}_h} \sum_{e \subset \partial K} \int_e \left(\boldsymbol{\nu}_e^T \mathbf{A} \nabla u_{\text{ACMS},B} + \boldsymbol{\nu}_e^T \mathbf{A} \nabla u_{\text{ACMS},\Gamma}\right) v_\Gamma\end{aligned}$$

and

$$\begin{aligned}a\left(u - u_{\text{ACMS}}, v\right) = &\sum_{K \in \mathcal{T}_h} \int_K \left[f - \mathcal{P}_{I_K}\left(f\right)\right]\left[v_{B,K} - \mathcal{P}_{I_K}\left(v_{B,K}\right)\right] \\ &+ \sum_{K \in \mathcal{T}_h} \int_K \left[f - \mathcal{P}_{I_K}\left(f\right)\right] v_\Gamma - \sum_{e \subset \Gamma} \int_e J_e\left(\boldsymbol{\nu}_e^T \mathbf{A} \nabla u_{\text{ACMS}}\right) v_\Gamma,\end{aligned}$$

where $J_e(\psi)$ denotes the jump of a given function ψ across the edge e in the direction $\boldsymbol{\nu}_e$. Next, we write

$$\begin{aligned}a\left(u - u_{\text{ACMS}}, v - v_{\text{ACMS}}\right) = &\sum_{K \in \mathcal{T}_h} \int_K \left[f - \mathcal{P}_{I_K}\left(f\right)\right]\left[v_{B,K} - \mathcal{P}_{I_K}\left(v_{B,K}\right)\right] \\ &+ \sum_{K \in \mathcal{T}_h} \int_K \left[f - \mathcal{P}_{I_K}\left(f\right)\right]\left(v_\Gamma - v_{\text{ACMS},\Gamma}\right) \\ &- \sum_{e \subset \Gamma} \int_e J_e\left(\boldsymbol{\nu}_e^T \mathbf{A} \nabla u_{\text{ACMS}}\right)\left(v_\Gamma - v_{\text{ACMS},\Gamma}\right),\end{aligned} \tag{B.3}$$

for all functions $v \in H_0^1\left(\Omega\right)$ and $v_{\text{ACMS}} \in V_{\text{ACMS}}$. Now the right hand side is bounded term by term to define an a posteriori error indicator.

First, on every element K, we have

$$\begin{aligned}&\int_K \left[f - \mathcal{P}_{I_K}\left(f\right)\right]\left[v_{B,K} - \mathcal{P}_{I_K}\left(v_{B,K}\right)\right] \\ &\qquad \leq \left\|f - \mathcal{P}_{I_K}\left(f\right)\right\|_{L^2(K)} \left\|v_{B,K} - \mathcal{P}_{I_K}\left(v_{B,K}\right)\right\|_{L^2(K)}\end{aligned}$$

ETNA
Kent State University
http://etna.math.kent.edu

and

$$\int_K [f - \mathcal{P}_{I_K}(f)] [v_{B,K} - \mathcal{P}_{I_K}(v_{B,K})] \leq \|f - \mathcal{P}_{I_K}(f)\|_{L^2(K)} \sqrt{\frac{\int_K (\nabla v_{B,K})^T \mathbf{A} \nabla v_{B,K}}{\lambda_{I_K,K}}}$$

or

$$\int_K [f - \mathcal{P}_{I_K}(f)] [v_{B,K} - \mathcal{P}_{I_K}(v_{B,K})] \leq \frac{\|f - \mathcal{P}_{I_K}(f)\|_{L^2(K)}}{\sqrt{\lambda_{I_K,K}}} \sqrt{\int_K (\nabla v)^T \mathbf{A} \nabla v}. \tag{B.4}$$

Before bounding the second and third terms of (B.3), $v_{\text{ACMS},\Gamma}$ is set as follows

$$v_{\text{ACMS},\Gamma} = E_\Omega \left(\mathcal{Q}(v_\Gamma) + \sum_{e \subset \Gamma} \Pi_{I_e} (v_\Gamma - \mathcal{Q}(v_\Gamma)) \right),$$

where the operator $\mathcal{Q}$ is the L^2-projection into the finite-dimensional subspace spanned by the piecewise linear functions on Γ.

On every element K, the second term of (B.3) is bounded,

$$\int_K [f - \mathcal{P}_{I_K}(f)] [v_\Gamma - v_{\text{ACMS},\Gamma}] \leq \|f - \mathcal{P}_{I_K}(f)\|_{L^2(K)} \|v_\Gamma - v_{\text{ACMS},\Gamma}\|_{L^2(K)}.$$

Define z as the unique solution in $H_0^1(K)$ of

$$-\nabla \cdot (\mathbf{A} \nabla z) = v_\Gamma - v_{\text{ACMS},\Gamma} \quad \text{in } K.$$

Since K is convex, the function z belongs to $H^2(K)$. We have

$$\begin{aligned} \|v_\Gamma - v_{\text{ACMS},\Gamma}\|_{L^2(K)}^2 &= \int_K (\nabla z)^T \mathbf{A} \nabla (v_\Gamma - v_{\text{ACMS},\Gamma}) \\ &\quad - \sum_{e \subset \partial K} \int_e \boldsymbol{\nu}_e^T \mathbf{A} \nabla z \, (v_\Gamma - v_{\text{ACMS},\Gamma}) \\ &= - \sum_{e \subset \partial K} \int_e \boldsymbol{\nu}_e^T \mathbf{A} \nabla z \, (v_\Gamma - v_{\text{ACMS},\Gamma}) \end{aligned}$$

because $v_\Gamma - v_{\text{ACMS},\Gamma}$ is an energy-minimizing extension. Next, we write

$$\|v_\Gamma - v_{\text{ACMS},\Gamma}\|_{L^2(K)}^2 \leq \sum_{e \subset \partial K} \|v_\Gamma - v_{\text{ACMS},\Gamma}\|_{H^{-\frac{1}{2}}(e)} \left\|\boldsymbol{\nu}^T \mathbf{A} \nabla z\right\|_{H^{\frac{1}{2}}(e)}. \tag{B.5}$$

For every edge $e \subset \partial K$, we have

$$\left\|\boldsymbol{\nu}^T \mathbf{A} \nabla z\right\|_{H^{\frac{1}{2}}(e)} \leq C_{\mathbf{A}} \|z\|_{H^2(K)} \leq C_{\mathbf{A}} \|v_\Gamma - v_{\text{ACMS},\Gamma}\|_{L^2(K)}.$$

Plugging this relation into (B.5), we get

$$\|v_\Gamma - v_{\text{ACMS},\Gamma}\|_{L^2(K)} \leq C_{\mathbf{A}} \sum_{e \subset \partial K} \|v_\Gamma - v_{\text{ACMS},\Gamma}\|_{H^{-\frac{1}{2}}(e)}.$$

ETNA
Kent State University
http://etna.math.kent.edu

The bound (A.4) on the projection error now yields

$$\|v_\Gamma - v_{\text{ACMS},\Gamma}\|_{L^2(K)} \leq C_{\varepsilon,\mathbf{A}} \sum_{e\subset\partial K} \frac{\|v_\Gamma - \mathcal{Q}\,(v_\Gamma)\|_{H^{\frac{1}{2}-\varepsilon}(e)}}{\lambda_{I_e,e}^{1-\varepsilon}}$$

with $0 < \varepsilon < \frac{1}{2}$. Using properties of the projection operator $\mathcal{Q}$ gives

$$\|v_\Gamma - v_{\text{ACMS},\Gamma}\|_{L^2(K)} \leq C_{\varepsilon,\mathbf{A}} \sum_{e\subset\partial K} \frac{h^\varepsilon}{\lambda_{I_e,e}^{1-\varepsilon}} |v_\Gamma|_{H^{\frac{1}{2}}(e)}\,;$$

see Steinbach [30, Eqn (12.19) on p. 271]. Using the continuity of the trace operator modifies the inequality as follows

$$\|v_\Gamma - v_{\text{ACMS},\Gamma}\|_{L^2(K)} \leq C C_{\varepsilon,\mathbf{A}} \|v_\Gamma\|_{H^1(K)} \left(\sum_{e\subset\partial K} \frac{h^\varepsilon}{\lambda_{I_e,e}^{1-\varepsilon}}\right).$$

The second term of (B.3) is bounded by

$$\begin{aligned}(\text{B.6})\quad &\int_K \left[f - \mathcal{P}_{I_K}(f)\right]\left[v_\Gamma - v_{\text{ACMS},\Gamma}\right] \\ &\qquad \leq C_{\varepsilon,\mathbf{A}} \|f - \mathcal{P}_{I_K}(f)\|_{L^2(K)} \|v\|_{H^1(K)} \left(\sum_{e\subset\partial K} \frac{h^\varepsilon}{\lambda_{I_e,e}^{1-\varepsilon}}\right).\end{aligned}$$

For every interior edge $e \subset \Gamma$, the third term of (B.3) satisfies

$$\begin{aligned}&\int_e J_e\left(\boldsymbol{\nu}_e^T \mathbf{A}\nabla u_{\text{ACMS}}\right)(v_\Gamma - v_{\text{ACMS},\Gamma}) \\ &\qquad \leq \left\|J_e\left(\boldsymbol{\nu}_e^T \mathbf{A}\nabla u_{\text{ACMS}}\right)\right\|_{L^2(e)} \|v_\Gamma - v_{\text{ACMS},\Gamma}\|_{L^2(e)}\,.\end{aligned}$$

Combining the bound (A.3) with $s = \frac{1}{2} - \varepsilon$ and properties of the projection operator $\mathcal{Q}$ yield

$$(\text{B.7})\qquad \|v_\Gamma - v_{\text{ACMS},\Gamma}\|_{L^2(e)} \leq C_{\varepsilon,\mathbf{A}} \frac{h^\varepsilon}{\lambda_{I_e,e}^{\frac{1}{2}-\varepsilon}} |v_\Gamma|_{H^{\frac{1}{2}}(e)}$$

where $0 < \varepsilon < \frac{1}{2}$.

Combining (B.3), (B.4), (B.6), and (B.7) gives

$$\begin{aligned}a\,(u - u_{\text{ACMS}}, v) \leq &\sum_{K\in\mathcal{T}_h} \frac{\|f - \mathcal{P}_{I_K}(f)\|_{L^2(K)}}{\sqrt{\lambda_{I_K,K}}} \sqrt{\int_K (\nabla v)^T \mathbf{A}\nabla v} \\ &+ C_{\varepsilon,\mathbf{A}} \sum_{K\in\mathcal{T}_h} \|f - \mathcal{P}_{I_K}(f)\|_{L^2(K)} \left(\sum_{e\subset\partial K\cap\Gamma} \frac{h^\varepsilon}{\lambda_{I_e,e}^{1-\varepsilon}}\right) \|v\|_{H^1(K)} \\ &+ C_{\varepsilon,\mathbf{A}} \sum_{e\subset\Gamma} \frac{h^\varepsilon}{\lambda_{I_e,e}^{\frac{1}{2}-\varepsilon}} \left\|J_e\left(\boldsymbol{\nu}_e^T \mathbf{A}\nabla u_{\text{ACMS}}\right)\right\|_{L^2(e)} |v_\Gamma|_{H^{\frac{1}{2}}(e)}\end{aligned}$$

ETNA
Kent State University
http://etna.math.kent.edu

for any function $v \in H_0^1(\Omega)$ and $\varepsilon > 0$. The Cauchy-Schwarz inequality implies

$$\begin{aligned}\frac{a(u-u_{\text{ACMS}},v)}{\sqrt{a(v,v)}} \leq C_{\varepsilon,\mathbf{A}} \Bigg\{ \sum_{K\in\mathcal{T}_h} \frac{\|f-\mathcal{P}_{I_K}(f)\|^2_{L^2(K)}}{\lambda_{I_K,K}} \\ + h^{2\varepsilon} \sum_{K\in\mathcal{T}_h} \|f-\mathcal{P}_{I_K}(f)\|^2_{L^2(K)} \left(\sum_{e\subset\partial K\cap\Gamma} \frac{1}{\lambda^{2-2\varepsilon}_{I_e,e}} \right) \\ + h^{2\varepsilon} \sum_{e\subset\Gamma} \frac{\left\| J_e\left(\boldsymbol{\nu}_e^T \mathbf{A}\nabla u_{\text{ACMS}}\right)\right\|^2_{L^2(e)}}{\lambda^{1-2\varepsilon}_{I_e,e}} \Bigg\}^{\frac{1}{2}},\end{aligned}$$

where we used

$$\sum_{K\in\mathcal{T}_h} \|v\|^2_{H^1(K)} = \|v\|^2_{H^1(\Omega)} \leq \frac{C}{\alpha_{\min}} \int_\Omega (\nabla v)^T \mathbf{A}\nabla v$$

and

$$\sum_{e\subset\Gamma} |v|^2_{H^{\frac{1}{2}}(e)} \leq \sum_{K\in\mathcal{T}_h} |v|^2_{H^{\frac{1}{2}}(\partial K)} \leq C \sum_{K\in\mathcal{T}_h} |v|^2_{H^1(K)} \leq \frac{C}{\alpha_{\min}} \int_\Omega (\nabla v)^T \mathbf{A}\nabla v.$$

The energy norm of the error $u - u_{\text{ACMS}}$ is bounded from above by a multiple of

$$\begin{aligned}\Bigg\{ \sum_{K\in\mathcal{T}_h} \frac{\|f-\mathcal{P}_{I_K}(f)\|^2_{L^2(K)}}{\lambda_{I_K,K}} + h^{2\varepsilon} \sum_{K\in\mathcal{T}_h} \|f-\mathcal{P}_{I_K}(f)\|^2_{L^2(K)} \left(\sum_{e\subset\partial K\cap\Gamma} \frac{1}{\lambda^{2-2\varepsilon}_{I_e,e}} \right) \\ + h^{2\varepsilon} \sum_{e\subset\Gamma} \frac{\left\| J_e\left(\boldsymbol{\nu}_e^T \mathbf{A}\nabla u_{\text{ACMS}}\right)\right\|^2_{L^2(e)}}{\lambda^{1-2\varepsilon}_{I_e,e}} \Bigg\}^{\frac{1}{2}}. \qquad \square\end{aligned}$$

REFERENCES

[1] T. ARBOGAST, *Mixed multiscale methods for heterogeneous elliptic problems*, in Numerical Analysis of Multiscale Problems, I. G. Graham, T. Y. Hou, O. Lakkis, and R. Scheichl, eds., vol. 83 of Lect. Notes Comput. Sci. Eng., Springer, Heidelberg, 2012, pp. 243–283.

[2] D. ARNOLD, L. SCOTT, AND M. VOGELIUS, *Regular inversion of the divergence operator with Dirichlet boundary conditions on a polygon*, Ann. Scuola Norm. Sup. Pisa Cl. Sci., 15 (1988), pp. 169–192.

[3] I. BABUŠKA, U. BANERJEE, AND J. E. OSBORN, *On principles for the selection of shape functions for the generalized finite element method*, Comput. Methods Appl. Mech. Engrg., 191 (2002), pp. 5595–5629.

[4] ———, *Generalized finite element methods—main ideas, results and perspective*, Int. J. Comput. Methods., 1 (2004), pp. 67–103.

[5] I. BABUŠKA, G. CALOZ, AND J. E. OSBORN, *Special finite element methods for a class of second order elliptic problems with rough coefficients*, SIAM J. Numer. Anal., 31 (1994), pp. 945–981.

[6] I. BABUŠKA AND J. E. OSBORN, *Generalized finite element methods: their performance and their relation to mixed methods*, SIAM J. Numer. Anal., 20 (1983), pp. 510–536.

[7] J. K. BENNIGHOF AND R. B. LEHOUCQ, *An automated multilevel substructuring method for eigenspace computation in linear elastodynamics*, SIAM J. Sci. Comput., 25 (2004), pp. 2084–2106.

[8] F. BOURQUIN, *Analysis and comparison of several component mode synthesis methods on one-dimensional domains*, Numer. Math., 58 (1990), pp. 11–33.

[9] ———, *Synthèse Modale et Analyse Numérique des Multistructures Élastiques*, Ph.D. Thesis, Université Paris VI, Paris, 1991.

[10] ———, *Component mode synthesis and eigenvalues of second order operators: discretization and algorithm*, RAIRO Modél. Math. Anal. Numér., 26 (1992), pp. 385–423.

[11] F. BREZZI AND L. D. MARINI, *Augmented spaces, two-level methods, and stabilizing subgrids*, Internat. J. Numer. Methods Fluids, 40 (2002), pp. 31–46.

ETNA
Kent State University
http://etna.math.kent.edu

[12] C.-C. CHU, I. G. GRAHAM, AND T.-Y. HOU, *A new multiscale finite element method for high-contrast elliptic interface problems*, Math. Comp., 79 (2010), pp. 1915–1955.

[13] R. CRAIG, JR. AND M. BAMPTON, *Coupling of substructures for dynamic analysis*, AIAA J., 6 (1968), pp. 1313–1319.

[14] W. E, B. ENGQUIST, X. LI, W. REN, AND E. VANDEN-EIJNDEN, *Heterogeneous multiscale methods: a review*, Commun. Comput. Phys., 2 (2007), pp. 367–450.

[15] Y. EFENDIEV AND T. Y. HOU, *Multiscale Finite Element Methods. Theory and Applications*, Springer, New York, 2009.

[16] P. GERVASIO, E. OVTCHINNIKOV, AND A. QUARTERONI, *The spectral projection decomposition method for elliptic equations in two dimensions*, SIAM J. Numer. Anal., 34 (1997), pp. 1616–1639.

[17] P. GRISVARD, *Elliptic Problems in Nonsmooth Domains*, SIAM, Philadelphia, 2011.

[18] M. HEATH, *Scientific Computing—An Introductory Survey*, McGraw-Hill, New York, 1997.

[19] P. HENNING, M. OHLBERGER, AND B. SCHWEIZER, *An adaptive multiscale finite element method*, Tech. Report 05/12, Angewandte Mathematik und Informatik, Universität Münster, 2012.

[20] U. HETMANIUK AND R. LEHOUCQ, *A special finite element method based on component mode synthesis techniques*, M2AN Math. Model. Numer. Anal., 44 (2010), pp. 401–420.

[21] T. Y. HOU AND X.-H. WU, *A multiscale finite element method for elliptic problems in composite materials and porous media*, J. Comput. Phys., 134 (1997), pp. 169–189.

[22] T. Y. HOU, X.-H. WU, AND Z. CAI, *Convergence of a multiscale finite element method for elliptic problems with rapidly oscillating coefficients*, Math. Comp., 68 (1999), pp. 913–943.

[23] W. C. HURTY, *Vibrations of structural systems by component-mode synthesis*, J. Engrg. Mech. Div., 86 (1960), pp. 51–69.

[24] M. JOHNSON AND U. HETMANIUK, *Spectrum and dispersion analyses for a special finite element discretization based on component mode synthesis*, in Proceedings of the 10th International Conference on Mathematical and Numerical Aspects of Waves, Vancouver, PIMS, Vancouver, 2011.

[25] B. KHOROMSKIJ AND G. WITTUM, *Numerical Solution of Elliptic Partial Differential Equations by Reduction to the Interface*, Springer, Berlin, 2004.

[26] J. M. MELENK, *On n-widths for elliptic problems*, J. Math. Anal. Appl., 247 (2000), pp. 272–289.

[27] J. NEČAS, *Sur les équations différentielles aux dérivées partielles du type elliptique du deuxième ordre*, Czechoslovak Math. J., 14 (1964), pp. 125–146.

[28] J. NOLEN, G. PAPANICOLAOU, AND O. PIRONNEAU, *A framework for adaptive multiscale methods for elliptic problems*, Multiscale Model. Simul., 7 (2008), pp. 171–196.

[29] A. QUARTERONI AND A. VALLI, *Domain Decomposition Methods for Partial Differential Equations*, Oxford University Press, New York, 1999.

[30] O. STEINBACH, *Numerical Approximation Methods for Elliptic Boundary Value Problems*, Springer, New York, 2008.

[31] A. TOSELLI AND O. WIDLUND, *Domain Decomposition Methods—Algorithms and Theory*, Springer, Berlin, 2005.